

Ultrafast Dynamics of Porphyrins in the Condensed Phase: II. Zinc Tetraphenylporphyrin[†]

Hua-Zhong Yu, J. Spencer Baskin, and Ahmed H. Zewail*

Laboratory for Molecular Sciences, Arthur Amos Noyes Laboratory of Chemical Physics, California Institute of Technology, Pasadena, California 91125

Received: February 11, 2002; In Final Form: April 17, 2002

Femtosecond spectroscopic studies of zinc tetraphenylporphyrin (ZnTPP) in benzene and dichloromethane are reported, combining both fluorescence up-conversion and transient absorption measurements. The purpose is to investigate the initial electronic and vibrational relaxation of the S_1 and S_2 excited states, in a system in which interference from solvent rearrangement is insignificant as evidenced by the small Stokes shift in the fluorescence. Excitation of the low-lying singlet excited state (S_1) results in nanosecond relaxation, while excitation to S_2 , the Soret band, leads to multiple electronic and vibrational relaxation time scales of S_2 and S_1 populations, from hundreds of femtoseconds to tens of picoseconds. The systematic and detailed studies reported here reveal that the Soret fluorescence band decays with a lifetime in benzene of 1.45 ps for excitation at 397 nm, while emission monitored at the same wavelength, but for two-photon 550 nm excitation, decays biexponentially with 200 fs and 1.0 ps time constants. In addition, the Soret fluorescence decay lifetime for 397 nm excitation is distinctly longer than the rise time of S_1 fluorescence for the same excitation, which varies with wavelength. These observations are consistent with the model presented here in which the Soret band structure consists of absorption from S_0 to two manifolds of states with distinct electronic and vibrational couplings to S_1 and higher electronic states. To compare with literature, we also measured the S_2 lifetime in dichloromethane and found it to be 1.9 ps, a lengthening from its value in benzene. However, the transient fluorescence intensity is greatly reduced. These observations in dichloromethane provide evidence of an ultrafast (<100 fs) channel for electron transfer from ZnTPP to dichloromethane for a subset of excited molecules in favorably oriented contact with the solvent, that is, a bifurcation of population. Finally, solvent-induced vibrational relaxation of the S_1 population following internal conversion from S_2 occurs over a range of time scales (picoseconds to tens of picoseconds) depending on the wavelength (fluorescence or transient absorption), and the observed rate indeed changes with solvent.

1. Introduction

Much research has been focused on understanding the spectroscopic and dynamic properties of metalloporphyrins because of their significance as biological reaction centers. As described in the preceding paper,¹ which is referred to henceforth as paper I, investigation of the ultrafast dynamics of cobalt porphyrins instigated our studies of free base tetraphenylporphyrin (H_2 TPP) and zinc tetraphenylporphyrin (ZnTPP) as reference systems. In paper I, the dynamics of H_2 TPP in benzene following excitation in the visible (Q_y and Q_x bands) and near-UV (Soret band) have been detailed. In this second paper, we report the results of a comparable study of ZnTPP. Both systems are very well-suited to experimental characterization of the vibrational relaxation process because the small Stokes shift of static fluorescence indicates an absence of significant solvent reorganization upon excitation.

The ground-state absorption and static emission properties of zinc porphyrin molecules have been well-established both experimentally and theoretically,^{2–4} along with the nanosecond relaxation dynamics of the low-lying excited S_1 state^{5,6} and millisecond time scale for luminescence from the lowest triplet state, T_1 .^{5,7} A common variant of the porphyrin macrocycle is produced by tetraphenyl substitution, and zinc tetraphenylporphyrin (ZnTPP) is no doubt one of the most extensively studied

porphyrin systems. The transient absorbance of S_1 (and T_1) ZnTPP was investigated in detail by means of picosecond transient absorption spectroscopy more than 1 decade ago.⁸ Excitation to the higher-lying S_2 excited state occurs via the Soret, or B, band, a very strong molecular absorption, which in ZnTPP is centered near 420 nm. In most porphyrins, rapid relaxation to S_1 follows S_2 excitation, and emission is dominated by the normal fluorescence from S_1 (in accord with Kasha's rule) and phosphorescence from T_1 .

Fluorescence from the S_2 state of a porphyrin was first observed 30 years ago for zinc tetrabenzoporphyrin, for which a picosecond fluorescence lifetime was inferred from the fluorescence yield and integrated absorption strength.⁹ Measurement of S_2 fluorescence of ZnTPP was first reported in 1975.¹⁰ In the 1980s, S_2 fluorescence quantum yields of ZnTPP were measured in various solvents^{11–14} and used to give estimates of the S_2 fluorescence lifetime ranging from 240 fs¹³ to 3.6 ps.¹¹ Line widths measured in a detailed study of the fluorescence excitation spectrum of ZnTPP seeded in a pulsed supersonic expansion of helium¹⁵ set a lower limit of 1 ps for S_2 relaxation in the isolated molecule.

In the 1990s, Chosrowjan et al.¹⁶ began the extension of ultrafast techniques to the study of ZnTPP dynamics, reporting S_2 fluorescence lifetimes of 3.5 and 0.75 ps for ZnTPP in acetonitrile and dichloromethane, respectively. On the basis of those measurements and a dependence of ZnTPP fluorescence yield on CH_2Cl_2 concentration when acetonitrile/ CH_2Cl_2 mix-

[†] Part of the special issue "Jack Beauchamp Festschrift".

tures were used as solvent, an effective intermolecular electron transfer from the S_2 state of ZnTPP to dichloromethane was suggested. The same year, separate spectral hole-burning experiments on ZnTPP in polymer matrixes doped with electron acceptors at cryogenic temperatures were reported by two groups,^{17,18} and opposite conclusions were reached on the question of electron transfer from the S_2 state. S_2 lifetimes ranging from 0.85 to 1.6 ps were also inferred from the hole line widths.¹⁸ Additional data supporting charge transfer from S_2 to CH_2Cl_2 is detailed in a recent review by Tokumaru.¹⁹

In 1998, Gurzadyan et al.²⁰ monitored the decay of the $S_2 \rightarrow S_0$ fluorescence and the rise of $S_1 \rightarrow S_0$ fluorescence for ZnTPP in ethanol using the fluorescence up-conversion technique and fit both to a single lifetime of 2.35 ps. These data, and measurements in other solvents by the same group,²¹ including a 2 ps S_2 lifetime for ZnTPP in CH_2Cl_2 , supported a simple picture of relaxation of an equilibrated S_2 population by internal conversion to S_1 . Further reports of ZnTPP S_2 relaxation lifetimes of 1.2 ps in CHCl_3 ²² and 1.6 ps in dimethyl formamide²³ have resulted from the application of transient absorption methods in conjunction with electron transfer or energy-transfer studies in zinc porphyrins and derivatized systems. In the first of these, a weak 18 ps component was also observed and attributed to vibrational cooling in the S_1 state following internal conversion from S_2 . This is similar to the ~ 10 ps time scale of vibrational cooling inferred from evolution of the transient absorption of a variety of different porphyrin systems under various excitation conditions.^{8,24} Very recently, Mataga et al.²⁵ used fluorescence up-conversion to explore the fluorescence from ZnTPP in ethanol over a wide wavelength range. Although their measurements showed the same 2.3 ps S_2 decay and S_1 rise as reported previously,²⁰ the fast rise of fluorescence at wavelengths in the wings of the S_1 , or Q band, emission required invoking a more complicated multistep dynamic process. Their interpretation, however, retained a first relaxation step of 2.3 ps from a single equilibrated S_2 population, followed by vibrational relaxation within the S_1 state on multiple time scales.

The femtosecond experiments that we report here on zinc tetraphenylporphyrin were carried out using two different techniques, fluorescence up-conversion and transient absorption. One- and two-photon visible excitation and UV excitation were employed with detection at a broad range of different wavelengths. Two solvents, benzene and dichloromethane, were used to examine the effect of the solvent and compare with the literature.

2. Experimental Section

The apparatus and procedures employed for the measurements reported here have been described in detail in paper I.¹ Briefly, the output of an amplified titanium–sapphire laser system was split into equal parts from which independently tunable pump and probe pulse trains were generated by nonlinear optical techniques. The pump pulse train was directed through a variable optical delay line and focused on the sample solutions in cells of 1 or 5 mm optical path length. The probe pulse either gated fluorescence collected from the sample or monitored the sample absorbance. In both cases, the measured signal was recorded as a function of delay line position, thus mapping the temporal response of the sample to the pump light pulse. Anisotropy effects were suppressed by setting the polarization axis for probe signal detection (of either emission or absorption) at 54.7° with respect to that of the pump. Comparison scans of cells containing pure solvent were recorded in conjunction with each set of experiments to ensure that the measurements were free of significant solvent-induced transients.

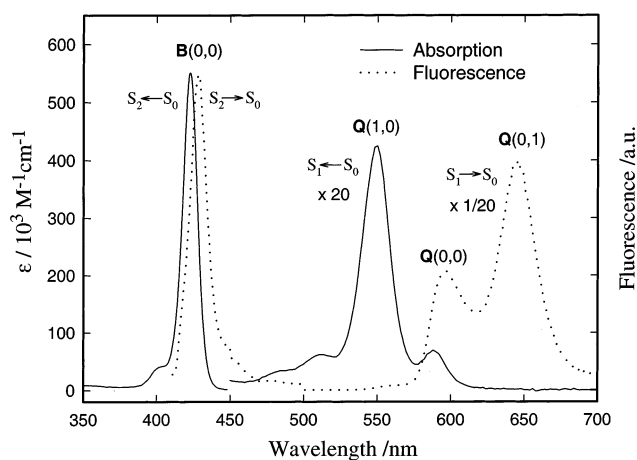


Figure 1. The ground-state absorption and static fluorescence spectra of ZnTPP in benzene. For the fluorescence spectrum, the excitation wavelength was 397 nm and the sample concentration was 1.2×10^{-7} M in a 5 mm cell.

For experiments in which ZnTPP in CH_2Cl_2 was excited at 397 nm in a 1 mm path length cell, immediate degradation of the sample was evident as a distinct greenish plume rising from the laser path through the cell. In this case, maintaining a flow of fresh sample into the irradiated volume was essential, and it was found that leaving the cell stationary and allowing convective transport of the heated photoproducts met this objective as effectively as rapid displacement of the cell.

The measured signals for both up-conversion and transient absorption were analyzed by fitting to a sum of exponential terms, $S(t) = \sum A_i \exp(-t/\tau_i)$, with independent amplitudes, A_i , and lifetimes, τ_i , using the minimum number of components required to leave no systematic deviation of the residual. Convolution with a Gaussian response function was included in the fitting procedure. The reported uncertainties in fit parameters are estimated 90% confidence limits based on reproducibility from fitting a number of independently measured transients.

Ground-state absorption and corrected static fluorescence spectra of the sample were obtained by using a UV–vis spectrometer (Cary, 50 Conc) and a fluorometer (ISA, FluoroMax-2). Uncorrected fluorescence spectra were also recorded using the femtosecond laser system. The absorption characterization of each sample was performed before and after use to check the quality of the sample throughout the course of the measurement.

Materials. The ZnTPP molecule was prepared and purified as described previously.²⁶ Benzene (EM Science, OmniSolv) and dichloromethane (EM Science, OmniSolv) were passed through a column of aluminum oxide (Aldrich, activated, basic, Brockmann I) before use. All experiments were carried out on aerated samples at ambient temperature ($\sim 24^\circ\text{C}$).

3. Results

Preliminary. Understanding the dynamic processes observed in the femtosecond measurements requires a clear idea of the static spectroscopic properties of the sample, which we therefore summarize here. Figure 1 displays absorption and fluorescence spectra of ZnTPP in benzene. The absorption spectrum consists of two strong bands, the B or Soret band and the Q band, traditionally identified as the $S_2 \leftarrow S_0$ and $S_1 \leftarrow S_0$ transitions.^{4,6,27–29} The peaks of these bands are assigned as B(0,0) and Q(1,0), where the number of quanta of the dominant Franck–Condon active vibrational mode in the excited state

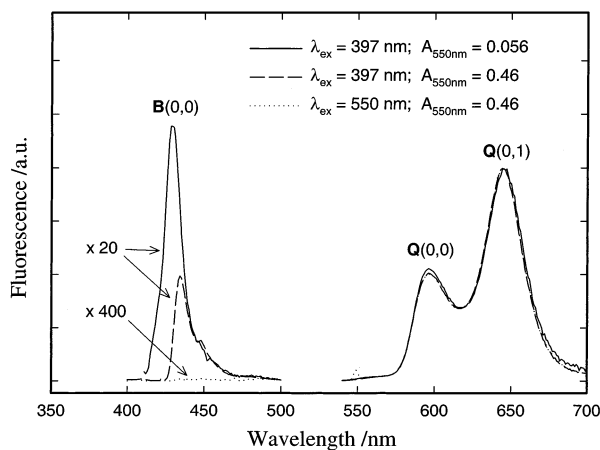


Figure 2. Comparison of static fluorescence spectra of ZnTPP in benzene for different concentrations and different excitation wavelengths. The two concentrations were 5.3×10^{-6} and 4.3×10^{-5} M. A 5 mm cell was used.

and in the ground state are given in parentheses.³⁰ These peaks are found in our spectra at 423 nm ($23\,640 \pm 80$ cm^{-1}) and 549 nm ($18\,210 \pm 50$ cm^{-1}), respectively. Additional features at 402, 510, and 589 nm are assigned to B(1,0), Q(2,0), and Q(0,0), respectively.³⁰ Agreement with spectra in the literature^{3,4,6,27–29} is good. The only excited-state lower than ${}^1\text{Q}(\pi, \pi^*)$ is ${}^3\text{T}(\pi, \pi^*)$ (or T_1).

The fluorescence spectrum in Figure 1 for 397 nm excitation clearly shows both $\text{S}_1 \rightarrow \text{S}_0$ and $\text{S}_2 \rightarrow \text{S}_0$ fluorescence. Peaks in S_1 fluorescence are measured at 596 nm for Q(0,0) and 645 nm for Q(0,1) with a shoulder at ~ 560 nm for Q(1,0), in good agreement with previous measurements,^{4,6,31} with relative peak intensities also in very good agreement with those of refs 4 and 31. The quantum yield of S_1 fluorescence is reported as 0.033⁴ or 0.03.³¹ The S_2 fluorescence peak of very dilute ZnTPP in benzene (1.2×10^{-7} M, 5 mm cell) for excitation at 397 nm is at 428.3 nm. S_2 fluorescence of ZnTPP in benzene at room temperature has been reported previously,¹² although the ratio of S_2 to S_1 fluorescence intensity in the published figure is not consistent with the reported relative fluorescence yield of $\varphi^{\text{S}_2}/\varphi^{\text{S}_1} = 0.012$. From the fluorescence spectrum in our Figure 1, $\varphi^{\text{S}_2}/\varphi^{\text{S}_1}$ can be determined to be 0.025 by integration of the respective fluorescence bands. The separation of fluorescence and absorption peaks in ref 12 also appears to be ~ 10 nm vs 5.6 nm in our spectra. A possible reason for these discrepancies will be addressed below. The lifetime for decay of S_1 , which occurs primarily by intersystem crossing to T_1 , is reported as 2.0 ns,¹² also measured in benzene at room temperature. The reported lifetime of T_1 measured at room temperature in outgassed solvents falls between 1 and 2 ms,^{7,11,32} while it increases to 23–26 ms in various deoxygenated solvents at 77 K.^{5,12,32}

Because of the extremely large extinction coefficient of $\text{S}_2 \leftarrow \text{S}_0$ absorption ($\epsilon_{423} = 5.44 \times 10^5$ M^{-1} cm^{-1})⁴ and the small Stokes shift (~ 300 cm^{-1}) and low quantum yield of S_2 fluorescence, reabsorption of emission can easily lead to distortion of the S_2 fluorescence band. This fact is demonstrated in Figure 2, in which the solid line and dashed line are fluorescence spectra for different sample concentrations in 5 mm cells. Normalization is based on the intensity of Q(0,1), for which reabsorption is negligible. There is little difference in the Q band structure, but the B band fluorescence of the concentrated sample (4.2×10^{-5} M) has a much lower intensity, and the peak is shifted to 434 nm. In the lower concentration sample (5.3×10^{-6} M), the fluorescence peak is also reduced

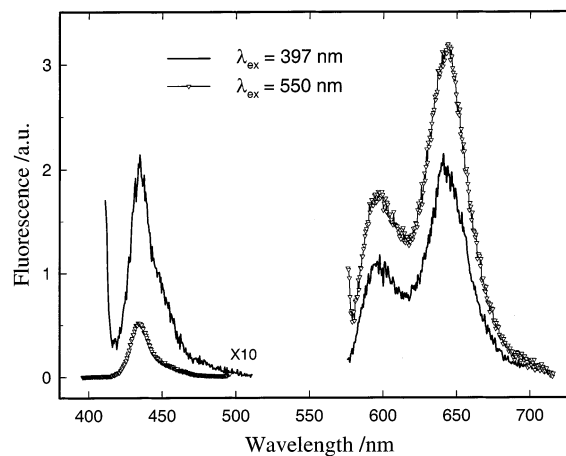


Figure 3. Uncorrected fluorescence spectra of ZnTPP in benzene following femtosecond laser excitation at 397 and 550 nm normalized to the number of absorbed photons. The concentration was 2.2×10^{-4} M in a 1 mm cell, and the pulse energy was 1.8 μJ at each pump wavelength. Both B band signals have been multiplied by a factor of 10.

(by $\sim 10\%$) and displaced (by ~ 1 nm) from the dilute sample limit. The $\varphi^{\text{S}_2}/\varphi^{\text{S}_1}$ ratio falls to 0.020 and 0.008 in these two spectra.

The change in the detected intensity of fluorescence from S_2 relative to that from S_1 as a function of concentration was reported earlier in a two-photon absorption study at similar concentrations³³ and suggested to arise from self-quenching. However, at the concentrations involved ($< 10^{-4}$ M), the diffusion-controlled bimolecular collision rate is orders of magnitude too low to produce dynamic quenching of the picosecond S_2 lifetime, and the peak shift that we observe is characteristic of the influence of reabsorption. To distinguish between quenching and reabsorption, spectra from cells of 1 mm and 5 mm path lengths were compared. It was found that absorbance rather than concentration was the determining parameter for the spectral changes, confirming the dominant role of reabsorption. To minimize reabsorption effects in the fluorescence spectrum of Figure 1, the sample was diluted to a maximum absorbance of 0.026 at 423 nm. The change in S_2 fluorescence peak position and yield ratio $\varphi^{\text{S}_2}/\varphi^{\text{S}_1}$ in ref 12 relative to the values obtained from our Figure 1 is suggestive of reabsorption, although it should account for only part of the discrepancy for their stated concentration of 2×10^{-6} M or less.

A plot of static fluorescence measured by the fluorometer for 550 nm excitation is also shown as a dotted line in Figure 2. It has the same Q band structure as that for S_2 excitation but shows no hint of B band fluorescence. Nevertheless, emission from the S_2 state of ZnTPP is easily observed upon pulsed laser excitation at 550 nm, as seen in Figure 3 and described previously.^{33,34} The two spectra shown in Figure 3, for excitation at 550 and 397 nm (both 1.8 $\mu\text{J}/\text{pulse}$), were recorded by removing the mixing crystal from our up-conversion setup and scanning the monochromator with no time-gating of the detected fluorescence other than the 10 ns boxcar integration window. The spectra are shown without spectral correction but are normalized by the total number of photons absorbed, which differed between the two excitations by only $\sim 10\%$. The B bands are adjusted in addition to compensate for changes in neutral density filter before the monochromator. Thus, the actual ratio of B band fluorescence intensities was roughly 4/1, as seen in the plots.

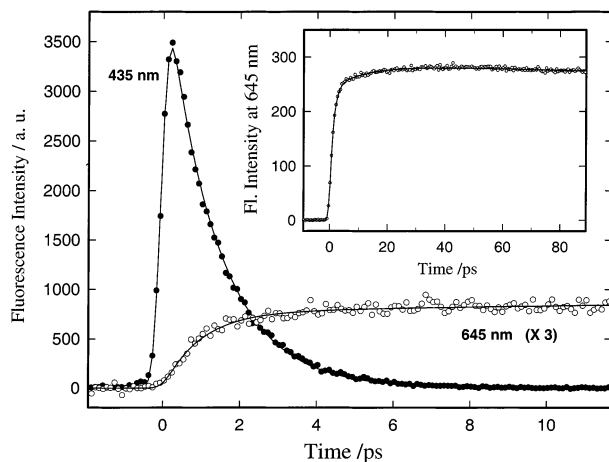


Figure 4. Fluorescence transients for 397 nm excitation of ZnTPP in benzene. Pump pulse energy was 0.9 μJ for the transients at 435 and 645 nm in the main figure. The inset shows a long time scale scan of 645 nm fluorescence using a cell with 5 mm path length at higher concentration ($A_{397} = 0.8$) and 2 μJ /pulse. Solid lines are fits of the experimental data.

The blue emission bands of the one-photon and two-photon spectra are very similar in shape, discounting the onset of laser scatter in the former at ~ 415 nm, albeit each is shifted by reabsorption like the high-concentration sample of Figure 2, which had a similar absorbance. Figure 3 shows that the two-photon laser excitation is very efficient, giving comparable S_2 fluorescence for similar absorbances and the same power at 397 and 550 nm. Tobita et al.³³ measured a high value of $1.8 \times 10^5 \text{ M}^{-1} \text{ cm}^{-1}$ for the molar extinction coefficient of the $S_n \leftarrow S_1$ absorption involved in the two-photon absorption pathway with 550 nm excitation. The similarities of the fluorescence spectra of Figure 3 also is reasonably interpreted as evidence that the emission for both excitation paths issues from a single excited-state manifold, commonly referred to as S_2 .

Another feature of Figure 3 that requires explanation is the difference in Q band intensities for identical detection conditions. With the applied normalization, a difference in the Q bands for excitation at 397 nm versus excitation at 550 nm can have two possible causes. The first is that all molecules from higher excited states do not relax via S_1 . The second possibility is that, because of two-photon absorption, the number of photons absorbed, which was measured, significantly misrepresents the number of molecules excited. Note, however, that correction for the two-photon absorption occurring at 550 nm would increase rather than diminish the normalized fluorescence intensity for 550 nm excitation and therefore amplify the observed discrepancy. Thus, if all higher excited states relax via S_1 , two-photon absorption at 397 nm must be substantial under the given excitation conditions. Further consideration will be given to this observation in the discussion.

Fluorescence Up-Conversion Measurements. Figure 4 shows the up-converted fluorescence profiles at two wavelengths for ZnTPP at low concentration ($A_{397} = 0.06$) in benzene with excitation of moderate power (0.9 μJ /pulse) at 397 nm. The signal from the solvent is very small at both wavelengths and does not interfere with the measurements. The 435 nm (S_2) fluorescence signal shows a rapid apparently monoexponential decay, while the 645 nm signal, corresponding to the peak of the static S_1 emission spectrum, shows a rise with two distinct components of about 1 and 10 ps and then decays on the nanosecond time scale.

The profile of the S_2 fluorescence of ZnTPP in benzene with excitation at 397 nm can be well fit as a single-exponential decay

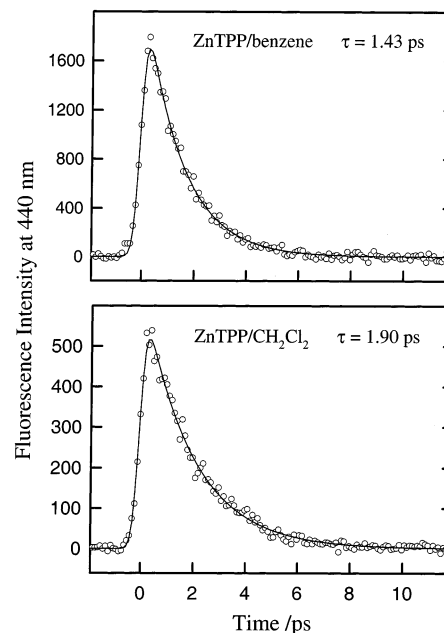


Figure 5. Comparison of 440 nm fluorescence for excitation at 397 nm (0.6 μJ /pulse) of ZnTPP in benzene ($A_{397} = 0.68$) and CH_2Cl_2 ($A_{397} = 1.0$). The intensity scales are as measured. Solid lines are fits of the experimental data with lifetimes, τ , as shown.

with a lifetime of 1.45 ± 0.10 ps (averaged over tens of experiments). No rise of S_2 emission was resolved in these experiments; however, we cannot exclude the possibility of a rise shorter than 200 fs such as that reported for ZnTPP in ethanol (60–90 fs).²⁰ The temporal behavior showed no dependence on pump power over the range of 70 nJ to 1.0 μJ per pulse. Also, no systematic dependence of the lifetime on fluorescence wavelength was found within the S_2 fluorescence band, from 427 to 445 nm, or even when measured at 500 nm. (A nanosecond fluorescence component of 5% relative amplitude was also measured at 500 nm.) However, a subtle departure from exponentiality was detected in the measurements, in which a fit of the tail of the signal typically yielded a lifetime ~ 0.1 ps longer than the full fit.

The dependence of the S_2 decay on solvent was also investigated. As shown in Figure 5, the decay lifetime of 440 nm fluorescence changed from 1.43 ps in benzene to 1.90 ps in CH_2Cl_2 , with all excitation and detection conditions held constant. The fluorescence intensity is much weaker in CH_2Cl_2 , although about 20% more photons were absorbed at 397 nm and reabsorption at 440 nm was reduced in CH_2Cl_2 relative to benzene because of a blue shift of the Soret band. Low-power excitation (0.6 μJ /pulse) was used to avoid any interference from two-photon absorption. Note that significant degeneration or decomposition of ZnTPP in CH_2Cl_2 is observed immediately upon irradiation with the 397 nm laser, which is in contrast to the very good stability of ZnTPP in benzene (no discernible spectral changes with 2 h laser irradiation at 397 nm and 2 μJ /pulse). A moderate reduction in measured intensity of the CH_2Cl_2 transient of about 30% was noted during the course of the experiment, evidently as a result of gradual sample depletion by the above-noted process.

As stated above, S_1 fluorescence for ZnTPP in benzene at 645 nm can be well fit with two distinct rise components, followed by a nanosecond decay. The fit parameters are given in Table 1 for fluorescence at 645 nm and several other wavelengths. The S_1 decay lifetime of ~ 1.7 ns measured over a time range of only 1.2 ns is in reasonable agreement with the

TABLE 1: Lifetimes and Relative Amplitudes of Up-Converted Fluorescence Measurements of ZnTPP in Benzene for Excitation at 397 nm

| λ_{fl} (nm) | lifetimes | | | relative amplitudes ^a | | | |
|----------------------------|---------------|---------------|---------------|----------------------------------|-------|-------|--------------------------|
| | τ_1 (ps) | τ_2 (ps) | τ_3 (ns) | A_1 | A_2 | A_3 | error limit ^b |
| 435 | 1.45 ± 0.10 | | | 1 | | | |
| 560 ^c | 0.2 ± 0.10 | 3.7 ± 1 | } 1.7 ± 0.2 | -1 | 0.7 | 0.1 | ±0.1 |
| 575 | 0.2 ± 0.10 | 5.5 ± 1.5 | | -1 | 0.6 | 0.4 | ±0.1 |
| 595–650 | 1.15 ± 0.10 | 12 ± 3.0 | | -0.84 | -0.16 | 1.0 | ±0.06 |
| 680 | 1.15 ± 0.10 | 12 ± 1.5 | | -1 | 0.24 | 0.76 | ±0.06 |

^a A negative amplitude indicates that the respective component is a rise instead of a decay. ^b Estimated 90% confidence limit in the amplitudes. ^c The 560 nm fluorescence was fit with a substantial (relative amplitude of 0.2) component of intermediate lifetime (~25 ps).

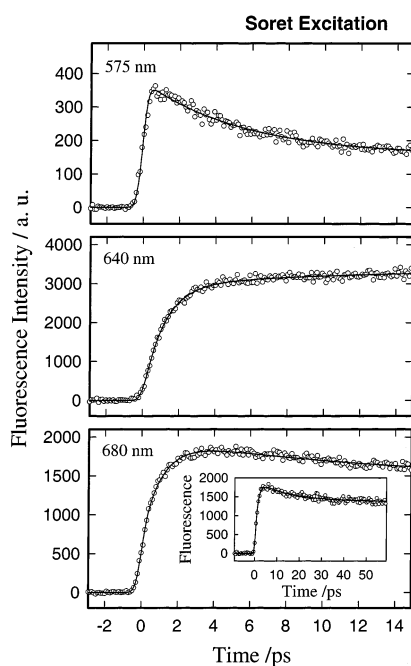


Figure 6. Q band fluorescence of ZnTPP in benzene. Excitation was at 397 nm; detection wavelengths were as indicated in the figure. Solid lines are fits of the experimental data (see Table 1).

2.0 ns lifetime reported by Ohno et al.,¹² which was measured for excitation with 2 ns pulses. For wavelengths of 595 nm and above, all fluorescence transients recorded at low power can be fit with a common pair of picosecond lifetimes. The dominant short lifetime in such a fit (1.15 ps) is distinguishably shorter than the S_2 decay (1.45 ps), while the smaller component fits to a lifetime of ~12 ps. Although the fast rise becomes even faster (down to as low as 0.8 ps) at higher pump power, the results in Table 1 apply for pump energies of ~0.2–1.0 μJ , for which the signal is linear with power. As was the case for the S_2 decay, this fast lifetime shows occasional signs of multiexponentiality, particularly for high-power excitation, for which enhanced contribution from a very fast component is suggested. The implications of this fact will be considered in the discussion.

As shown in Figure 6 and indicated in Table 1, the relative amplitudes of the picosecond components can be altered by changing the wavelength of fluorescence detection. In particular, fluorescence measured at 680 nm, in the long wavelength tail of the Q(0,1) fluorescence band, has the second component appearing as a decay. In the previous femtosecond ZnTPP S_1 fluorescence measurements,^{20,21,25} only a single exponential rise was reported at the Q(0,0) fluorescence peak, but the signal/noise ratios may not have been high enough to identify a longer component of relative amplitude similar to that observed here. A completely different form of fluorescence transient is measured below 580 nm, with a full rise no longer than a few

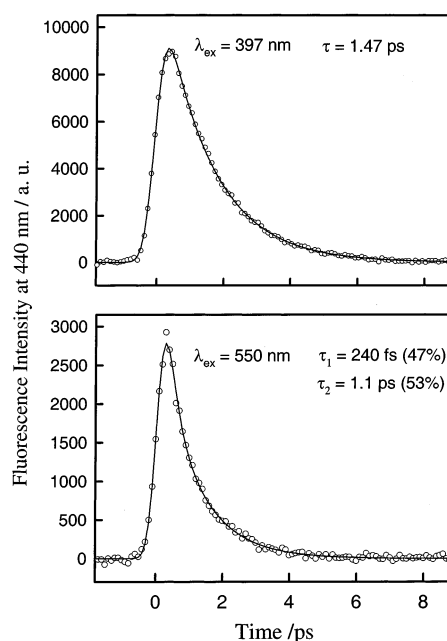


Figure 7. Comparison of 440 nm fluorescence of ZnTPP in benzene for two excitation wavelengths: 397 nm (1.5 μJ /pulse) and 550 nm (2.0 μJ /pulse). The intensity scales are as measured. Solid lines are fits of the experimental data with lifetimes as shown.

hundred femtoseconds and dominant decays of a few picoseconds before the 1.7 ns component. In the weak fluorescence at 560 nm, an additional small decay component of ~25 ps is indicated. Qualitatively similar transients were measured in ref 25 for wavelengths between 500 and 600 nm, showing rises much faster than the 2.3 ps decay of S_2 in ethanol.

As shown in Figure 3, emission at 440 nm can also be produced by a two-photon process for moderately intense 550 nm excitation. We investigated the temporal evolution of this fluorescence by up-conversion and found that it differs from that observed under identical detection conditions for excitation at 397 nm. Figure 7 shows two transients, recorded consecutively with only a change in the pump wavelength and energy, and their fits. The specific fit parameters are given in the figure. The signal for 397 nm pump wavelength is a single exponential; for 550 nm, there is again no measurable rise in the signal but now a biexponential decay with lifetimes much faster than the decay observed for excitation at 397 nm. Note that there is no solvent response contribution to the fast transient. The dependence of the intensity of this fluorescence signal on the 550 nm laser power is quadratic for excitation at low power density ($<1 \times 10^{15}$ photons cm^{-2} pulse⁻¹ or ~0.8 μJ /pulse at our focusing), as expected for fluorescence of two-photon origin, but the transient shape is independent of the pump power from 0.3 to 3 μJ /pulse.

TABLE 2: Lifetimes and Relative Amplitudes of the Pump–Probe Transient Absorption Dynamics of ZnTPP in Benzene and Dichloromethane for Excitation at 397 nm

| Lifetimes (all λ) | | | | | | |
|----------------------------|------------------|-----------------|---------------------------------------|---------------------------------------|-----------------|-----------------|
| ZnTPP/benzene | | | ZnTPP/CH ₂ Cl ₂ | | | |
| τ_1 (ps) | τ_2 (ps) | | τ_1 (ps) | τ_2 (ps) | | |
| 1.5 \pm 0.2 | 12 \pm 3.0 | | 2.1 \pm 0.3 | 38 \pm 5.0 | | |
| Amplitudes | | | | | | |
| λ probe (nm) | ZnTPP/benzene | | | ZnTPP/CH ₂ Cl ₂ | | |
| | A_1^a | $A_2^{a,b}$ | A_3^c | A_1^a | A_2 | A_3^c |
| 571 | -0.29 | (-0.05) | 1.0 | -0.14 | 0.42 \pm 0.05 | 0.58 \pm 0.07 |
| 590 | -0.08 \pm 0.02 | 0.08 \pm 0.02 | 0.92 | 0.13 | 0.39 \pm 0.05 | 0.48 \pm 0.04 |
| 620 | 0.28 | | 0.72 | | | |
| 638 | 0.55 | 0.08 | 0.37 | | | |
| 656 | 0.71 \pm 0.08 | 0.11 \pm 0.02 | 0.18 | 0.50 | 0.32 \pm 0.05 | 0.18 \pm 0.02 |
| 682 | 0.39 | (-0.05) | 0.61 | | | |
| 702 | 0.33 | (0.05) | 0.62 | | | |

^a A negative amplitude indicates that the respective component is a rise instead of a decay. ^b A_2 values are placed in parentheses when the presence of a τ_2 component is not certain. ^c A_3 is the amplitude of the plateau reached when the first two components have effectively disappeared with the sum of positive amplitudes normalized to 1.

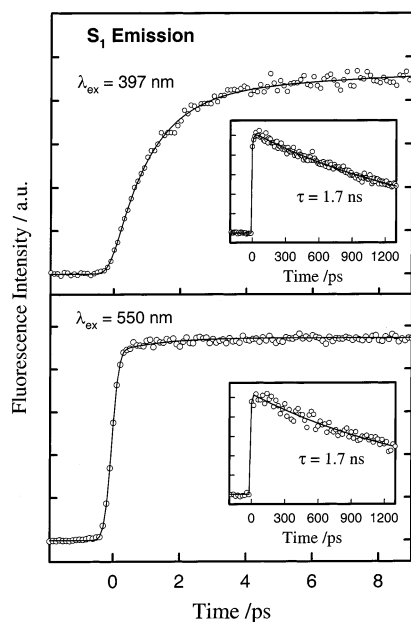


Figure 8. Comparison of Q band fluorescence of ZnTPP in benzene for two excitation wavelengths: 397 and 550 nm. The fluorescence wavelengths are 650 and 635 nm, respectively. The insets show the same signals on the nanosecond time scale. Solid lines are fits of the experimental data. The early time data for $\lambda_{\text{ex}} = 550$ nm is fit with a 3% rise of 1 ps lifetime and a 4% rise of 12 ps lifetime.

S_1 fluorescence was also measured for 550 nm excitation. In contrast to the slow full rise (≥ 1 ps) with excitation at 397 nm, the femtosecond system response accounts for more than 90% of the rise observed upon excitation at 550 nm (Figure 8). At the pump power used for the 550 nm data in Figure 8 (2 $\mu\text{J}/\text{pulse}$), a slight biexponential rise (see caption) can be detected after the response, corresponding to relaxation of the higher excited states resulting from two-photon excitation. On the nanosecond time scale, the S_1 fluorescence signal shows the usual 1.7 ns decay, regardless of the excitation pathway (see Figure 8 insets).

Transient Absorption Measurements. Figure 9 displays the femtosecond transient absorption profiles of ZnTPP in benzene at three representative wavelengths when pumping at 397 nm. For each, measurements of benzene alone showed negligible

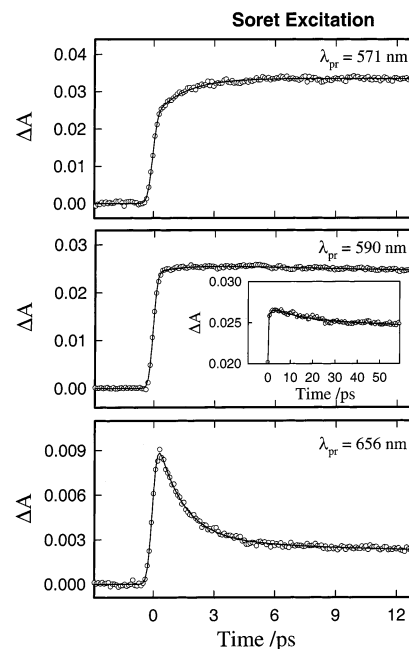


Figure 9. Femtosecond transient absorbance of ZnTPP in benzene. Pump wavelength was 397 nm; probe wavelengths were as shown. Absorbance in the 1 mm cell at the pump wavelength was 0.55 (sample concentration $\approx 2.2 \times 10^{-4}$ M), and the ΔA axes are adjusted for variations in pump power to be directly comparable. Solid lines are fits of the experimental data (see Table 2).

solvent contribution to the signal. In all cases, the transient absorption has a long-lived (\geq nanosecond) contribution, which may either decay or rise with the 1.7 ns S_1 lifetime to another much longer-lived plateau, depending on the relative absorption strengths of S_1 and T_1 at the probe wavelength employed.⁸ The total transient absorption signals shown in Figure 9 were well fit with at most two picosecond exponential components (lifetimes 1.5 and 12 ps) in addition to the nanosecond and longer behavior. The fit parameters are given in Table 2. For simplicity, only the plateau amplitude reached on a time scale of 100–200 ps is given in the table, rather than a full characterization of the long time evolution, which is beyond the scope of interest here. However, this evolution has been given consideration in the fitting to check for any influence on the parameters extracted for the short time behavior.

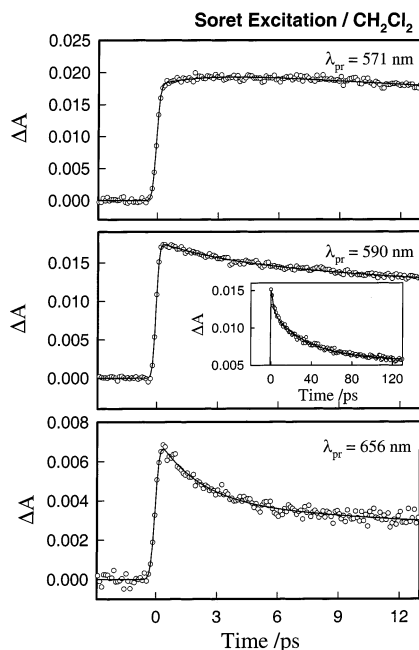


Figure 10. Femtosecond transient absorbance of ZnTPP in CH_2Cl_2 . Pump wavelength was 397 nm; probe wavelengths were as shown. Absorbance in the 1 mm cell at the pump wavelength was ~ 1.1 , and the ΔA axes are adjusted for variations in pump power to be directly comparable. Solid lines are fits of the experimental data (see Table 2).

As seen in Figure 9 and indicated in Table 2, the relative amplitudes of the 1.5 ps component depends strongly on the probe wavelength, changing from a rise at 571 and 590 nm to a decay at 620 nm and above, achieving its maximum relative amplitude when probing near 656 nm. When clearly resolved, the second lifetime is a decay but appears to enter as a very weak rise at 571 and 682 nm. At shorter wavelengths investigated (470–480 nm), neither lifetime was apparent (i.e., the signal is flat to within $\sim 2\%$ after a response limited rise). When the pump wavelength was tuned to 416 nm, there was no noticeable change in the transient behavior. At a probe wavelength of 646 nm, a 1.5 ps component was dominant (60%), very similar to the bottom transient of Figure 9.

The transient absorption at three probe wavelengths using CH_2Cl_2 as solvent is shown in Figure 10 with fit parameters given in Table 2. The dynamic profiles of ZnTPP in CH_2Cl_2 are generally similar in appearance to those in benzene, with the major difference being the much greater relative amplitude and much longer lifetime (38 vs 12 ps) of the second picosecond component. The shortest lifetime also becomes slightly longer (2.1 vs 1.5 ps), consistent with the change in the measured S_2 fluorescence lifetime.

Transient absorption of ZnTPP in benzene was also measured following S_1 excitation at pump wavelengths from 530 to 590 nm. The transients generally rose with the system response to a plateau, which remained flat to within a few percent on the picosecond time scale. When probing in the vicinity of 656 nm, however, a ~ 1.4 ps decay component could be easily observed because of a two-photon absorption contribution. For excitation with 2 $\mu\text{J}/\text{pulse}$, for example, this component reached an amplitude of 25% of the total ΔA .

4. Discussion

The successive relaxation steps of excited ZnTPP are most clearly resolved in the measurements of fluorescence from S_1 and S_2 . The same rates, although somewhat less-well-determined

because of overlap of the absorptions of the various populated excited states, are observed in our transient absorption measurements. The broad picture confirms general features of the ultrafast dynamics that can be inferred from an array of previous studies in other solvents:^{20–23} for excitation around 400 nm, relaxation of S_2 by internal conversion (IC) and the rise of S_1 occur in about 1–2 ps, followed by a slower vibrational relaxation by energy loss to the solvent on a time scale on the order of 10 ps.

Although this qualitative picture is upheld, the present results show features that indicate greater complexity in the dynamics than the above description suggests. These features are two in number: (1) the time evolution of Soret band fluorescence is dramatically different for excitation at 550 nm than for excitation at 397 nm; (2) when exciting at 397 nm, the decay of S_2 fluorescence is slower than the initial rise of S_1 fluorescence, distinctly so in the blue tail of the emission ($\lambda < 580$ nm), but also consistently so at the peak of the S_1 fluorescence spectrum, when each is fit to a single-exponential lifetime. (Because the uncertainty in rise time for any given transient at the S_1 fluorescence peak exceeds 0.2 ps, we only became convinced of the significance of the difference with the S_2 decay time of 1.45 ± 0.1 ps by the consistency of the observation over many repetitions. Note, however, that this difference is not essential to our arguments below.)

The observation of the fast rise of S_1 fluorescence below 600 nm was recently reported by Mataga et al. for excitation of ZnTPP in ethanol at 405 nm.²⁵ The interpretation given there involved a monoexponential decay from a single higher excited state (S_2) to high-lying vibrational levels of S_1 , followed by fast vibrational relaxation in the S_1 state. It was proposed that, because a rapidly decaying population can be observed to rise with its own lifetime, fluorescence from the vibrationally hot levels could produce the rapidly rising fluorescence signals. While this is theoretically possible if a specific, fortuitous balance between the detection cross-sections of the intermediate and of the relaxed S_1 populations were to exist, our observation of a rise at the S_1 fluorescence peak that is faster than the Soret decay and the strong and rapidly decaying fluorescence at 440 nm under two-photon excitation cannot be explained by this postulate.

However, all of the observations can be explained by the existence of a second distinct electronic potential surface in close proximity to S_2 , which has significant absorption from S_0 . We note that, although the excited state generated by all excitation in this spectral region has been generally denoted as S_2 in the literature,^{11,16,20–23,30,35} in fact, it is a matter of question whether absorption near 400 nm, which is about 1400 cm^{-1} above $B(0,0)$, can be solely attributed to vibrational excitation of the ${}^1B(\pi, \pi^*)$ state.³⁵ Both B and Q are doubly degenerate states for 4-fold symmetric metalloporphyrins in Gouterman's four-orbital model.³⁰ However, femtosecond decays of the anisotropy following coherent excitation of the Q bands of MgTPP³⁶ confirm the negligible splitting and strong interaction of Q_x and Q_y states. Because neither two degenerate and strongly coupled upper states nor a single S_2 state decaying by two distinct parallel channels (as to Q_x and Q_y) would allow detection of the separate and distinguishable S_2 decay rates that we observed, we believe our results are related not to degenerate states but to two independent and at most weakly coupled states, which we will designate S_2 and S_2' . Nonetheless, studies of electronic degeneracies of related metalloporphyrins^{36,37} could be relevant to the electronic relaxation pathways elucidated here.

If the higher lying of the two postulated states is denoted as S_2' , we may interpret the current experimental results to establish the following characteristics of the two states. First, S_2 decays with a single time constant of 1.45 ps, while S_2' decays biexponentially with a fast 200 fs initial depopulation. Second, both states are populated by absorption at 397 nm, while absorption of two photons of 550 nm light leads almost exclusively to S_2' by relaxation from higher-lying states. Third, following 397 nm excitation, the relative contribution of S_2 to the fluorescence measured from 430 to 440 nm is greater than its relative contribution to population of S_1 via IC, as evidenced by the measured effective rise of 1.15 ps at the S_1 fluorescence peak.

This last characteristic is interpreted to arise from the blue shift of the S_2' fluorescence maximum relative to that of S_2 so that, given the concentrations at which the femtosecond experiments were performed, the wavelengths detected to avoid severe reabsorption precluded detection of significant S_2' fluorescence. Even for experiments in which the absorbance at 397 nm was as low as 0.05, the absorbance at 423 nm was ~ 1.0 and the measured transient for fluorescence at this wavelength was distorted by reabsorption and contaminated by scattered light. Thus, the time dependence of fluorescence at wavelengths shorter than about 427 nm, accounting for almost half of the emission induced by 397 nm excitation, was not determined. If this interpretation is correct, it may be possible to increase the relative population of S_2 over S_2' by tuning the excitation wavelength to the red, thereby changing the S_1 fluorescence transients. Such an experiment has not been attempted.

A second possibility for a contribution by S_2' to the S_1 rise that is greater than its contribution to the observed Soret fluorescence decay is that a major pathway for S_2 relaxation bypasses S_1 , going directly to T_1 or S_0 . This initially appeared to be supported by the experiments of Figure 3, suggesting that S_1 fluorescence yield for 397 nm excitation is lower than that for 550 nm excitation, and that, therefore, a substantial segment of the excited population, which could derive predominantly or exclusively from S_2 , does not relax via S_1 . However, the evidence of porphyrin S_1 fluorescence excitation spectra indicates that all excited-state populations return to S_1 with close to 100% yield.¹² When this is accepted, the S_1 fluorescence discrepancy in Figure 3 must rather indicate a high efficiency for two-photon absorption at 397 nm, even at moderate pulse energies.

In Figure 11, we represent schematically the major points of the above description. One quanta of the principal Franck–Condon active mode is represented above the ground-state level of the S_1 and S_2 electronic states. Both S_2 and S_2' are populated by the 397 nm excitation. Only S_2' is populated by relaxation in less than 100 fs from the higher-lying state reached by absorption of two 550 nm photons (not shown).

The biexponential decay from S_2' with a 200 fs initial component is reminiscent of the recently measured relaxation dynamics of S_1 azulene.³⁸ The femtosecond time scale suggests that some of the population proceeds coherently via a conical intersection to the S_1 potential, with the remaining population leaking out more slowly. From S_2 , a quasi-statistical IC occurs at a total rate of $(1.45 \text{ ps})^{-1}$ via coupling to the dense S_1 vibrational manifolds. Because the initial population in S_2 is not in equilibrium with the solvent, it is reasonable that over the course of the several picoseconds that this population persists, there is some change in decay rate, though we see only a very small rate decrease.

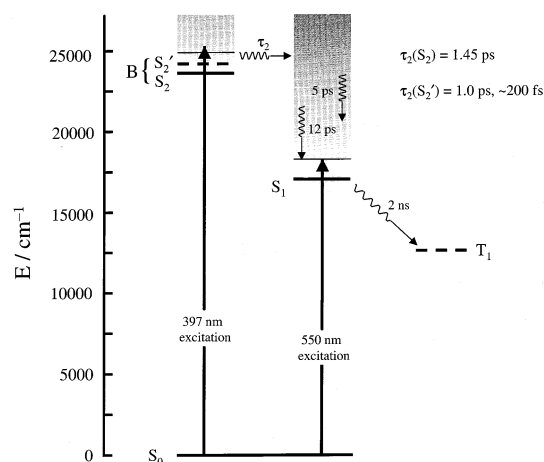


Figure 11. Schematic diagram of the energy relaxation dynamics of ZnTPP. Solid horizontal lines are located at the energies of bands in the absorption spectrum. Dashed lines indicate approximate energies for S_2 and T_1 . See text for details of the dynamics.

Those molecules that relax from S_2 and S_2' to S_1 have about 8000 cm^{-1} of excess vibrational energy. In paper I, H_2TPP internal conversion in $\sim 50 \text{ fs}$ created an S_1 population with a vibrational state distribution determined by the specific inter-electronic couplings of the molecular Hamiltonian. This distribution then relaxed by a hierarchy of intra- and intermolecular vibrational processes. Similar fast electronic relaxation ($\leq 150 \text{ fs}$) has been recently observed in both the free base and zinc complex of a different porphyrin in benzene solution.³⁹ In contrast, the relatively slow rise of S_1 population for ZnTPP ($\sim 1 \text{ ps}$) becomes the rate-determining step, which obscures the stages of spontaneous and elastic-collision-induced intramolecular vibrational relaxation that were seen in H_2TPP . Thus, on the time scale of S_1 formation, the 8000 cm^{-1} of excess vibrational energy is randomly distributed among the internal vibrational modes of the ZnTPP molecule, leaving it above the temperature of the solvent bath.

For a molecule of the size of ZnTPP, with hundreds of vibrational modes, 8000 cm^{-1} is only enough energy to raise the occupation number in the Franck–Condon active coordinate by one quanta ($\sim 1250 \text{ cm}^{-1}$) in a small fraction of molecules. Thus, the rise of S_1 fluorescence at the wavelengths of the static fluorescence bands occurs as the S_1 state is populated, which must have contributions at 200 fs and 1 ps from S_2' relaxation and 1.4 ps from S_2 IC. These lifetimes are close enough together that the rise can be fit as a single exponential of 1.15 ps, as confirmed by fits of simulated data. At moderate to high pump powers, many molecules excited to S_2 absorb a second photon, as demonstrated by Figure 3. As we have shown, the relaxation from higher excited states reached by two-photon absorption at 550 nm is predominantly via S_2' ; it is not unexpected, then, that as 397 nm excitation power is increased the faster rising contribution to S_1 fluorescence increases and the total rise time grows shorter. Fluorescence at 560 and 575 nm rises on a time scale ($\sim 200 \text{ fs}$) similar to that of the fast decay from S_2' . That it is seen clearly here suggests that passage through the conical intersection leads preferentially to part of the S_1 manifold with relatively strong emission at this wavelength.

The final slow (5–40 ps) intensity changes correspond to changes in Franck–Condon factors for relaxation of one or two quanta of the active mode by loss of excess vibrational energy to the solvent. Our results show vibrational cooling of the Q state on multiple time scales, as previously observed in transient absorption studies on nickel porphyrins.⁴⁰ Note that the effective

cooling rates of $(5 \text{ ps})^{-1}$ and $(12 \text{ ps})^{-1}$ (in benzene) characterize different regions of the S_1 vibrational manifold rather than sequential relaxation steps, as indicated in Figure 11. From the wavelength dependence of our fluorescence up-conversion measurements (Figure 6), we see that the fluorescence spectrum is narrowing, as expected from Franck–Condon considerations, by a settling of the population in an S_1 potential displaced from S_0 . Similar spectral narrowing of fluorescence by vibrational cooling has been reported for DCM in CHCl_3 and methanol, for example.⁴¹

The mean cooling lifetime of $\sim 12 \text{ ps}$ in benzene becomes much longer when CH_2Cl_2 is used as the solvent. This may be understood as resulting from a poor frequency match between the instantaneous normal modes of the solvent and the Franck–Condon active mode.⁴² The slow decay component also appears as a much larger fractional contribution to the transient absorption signal in CH_2Cl_2 . This is most likely due to changes in the Franck–Condon overlap of S_1 with the absorbing state, because the intramolecular energy redistribution, which produces the initial hot vibrational distribution in S_1 , should not depend strongly on the solvent. In CHCl_3 , the only other solvent in which vibrational cooling has been reported, an 18 ps lifetime was observed (pumping at 400 nm and probing at 610 nm).²²

In changing the solvent from benzene to CH_2Cl_2 , the lifetime of the S_2 fluorescence lengthens to 1.9 ps, in agreement with the lifetime of 2.0 ps reported by Gurzadyan et al.²¹ for excitation at 394 nm. This change in lifetime is also consistent with the suggested relation of IC rate to the solvent-dependent S_2 – S_1 energy gap,^{18,21} which changes from $\sim 6670 \text{ cm}^{-1}$ in benzene to 6800 – 6900 cm^{-1} in CH_2Cl_2 .^{28,29} This result appears to be at odds, however, with the S_2 fluorescence lifetime of 750 fs reported by Chosrowjan et al.¹⁶ for excitation at 410 nm. We saw no effect on transient absorption rates of ZnTPP in benzene upon changing the excitation from 397 to 416 nm, and we do not consider an accelerated decay for lower-energy excitation in CH_2Cl_2 to be a likely explanation for the discrepancy. Because the experiments of ref 16, as a result of the sample concentration, path length, and choice of detection wavelength, were subject to a severe reabsorption effect, the up-conversion signals were clearly distorted and may not be reliable. As we have noted here, Soret band fluorescence for ZnTPP in benzene is observed to decay as fast as 200 fs when excitation occurs by two-photon absorption, so a fast rate may also reflect substantial two-photon contributions.

The efficient degradation of ZnTPP in CH_2Cl_2 following excitation to S_2 , but not to S_1 , is well-known.^{16,17,19} The measured S_2 lifetime (1.9 ps), which is close to but longer than that in benzene, DMSO,²¹ toluene,²¹ CHCl_3 ,²² and DMF,²³ cannot be cited as support for the existence of a fast channel for electron transfer to solvent from the S_2 state, especially because the isolated molecule lifetime is inferred to be $\sim 1 \text{ ps}$;¹⁵ hence, the solvent effect on intramolecular relaxation is weak. However, the substantial reduction in initial S_2 fluorescence amplitude relative to benzene, given that the radiative rate varies only marginally with solvent,⁴³ clearly indicates a direct reaction from the S_2 state, consistent with the previous observations of quenching of S_2 fluorescence as a function of CH_2Cl_2 concentration in acetonitrile.^{16,19}

It is important to note, however, that interpretation of the quenching of fluorescence intensity in terms of a single bimolecular reaction rate (dynamic quenching) is not valid in this situation. With time resolution of the order of 100 fs, we see a difference of at least a factor of 3 in the earliest measurable fluorescence intensity, after taking into consideration absorption,

reabsorption, and sample degradation. Thus, two-thirds or more of the population excited by the excitation pulse disappears from the excited state in less than 100 fs, while the decay rate of the remaining molecules is that of a typical ZnTPP IC from S_2 to S_1 . This fact indicates that the quenching is not dynamic but results from the existence of a distribution of solute–solvent structures in the solution that are static over the S_2 lifetime and exhibit different electron-transfer rates.

Under favorable mutual orientation, electron transfer from ZnTPP to the solvent is faster than 100 fs, while for the remaining population it is much slower than 2 ps. Changing the CH_2Cl_2 concentration in the mixed solvent does not change these rates; rather, it shifts the equilibrium that exists between those ZnTPP molecules that are in favorably oriented ZnTPP– CH_2Cl_2 structures and those that are not (including those in unfavorable complexes and those with large solute– CH_2Cl_2 separations), thereby changing the quenching yield. The proposed 15 Å quenching radius from the mixed solvent study¹⁹ therefore reflects an average distance for formation of complex with favorable geometry. A similar case of the dependence of fluorescence yield on static, conformation-controlled quenching without a commensurate dependence of the measurable rate has been observed in this laboratory in quenching of the fluorescence of ethidium intercalated in DNA.⁴⁴

5. Conclusion

In this paper, we reported our femtosecond spectroscopic study of the relaxation dynamics of zinc tetraphenylporphyrin (ZnTPP). With the use of femtosecond-resolved fluorescence up-conversion and pump–probe transient absorption techniques, the dynamics of ZnTPP in different solvents were examined upon excitation at 397 and 550 nm. From these observations, we provide a dynamical model for the intramolecular processes and for the effect of the solvent on vibrational relaxation and intermolecular electron transfer; solvation of excited porphyrin is insignificant and no dynamical Stokes shift was observed.

Of particular interest is the structure of the Soret absorption; we suggest two excited state manifolds with overlapping absorptions at 397 nm, which exhibit different relaxation dynamics. The contribution of a second electronic state to the Soret band absorption had not previously been demonstrated. Internal conversion from these higher electronic states to Q (or S_1), with time constants from 200 fs to 1.45 ps, is much slower than that in H_2TPP in which it is complete within $\sim 50 \text{ fs}$.

The Q state lives for nanoseconds, but when populated by internal conversion from higher-lying states, it loses excess vibrational energy to the solvent in tens of picoseconds. Our results also support the existence of an ultrafast electron transfer from ZnTPP in the S_2 state to dichloromethane solvent when the two molecules are in favorable mutual orientation, which has been a matter of dispute in the literature. This picture is also supported by a recent study⁴⁵ (published in the proofs stage of the present work) showing similar inhomogeneous ultrafast charge separation in other solvents.

Acknowledgment. This work was supported by the National Science Foundation (Laboratory for Molecular Sciences). We thank Prof. Fred Anson for discussions that we had in this and related collaborative research.

References and Notes

- (1) Baskin, J. S.; Yu, H.-Z.; Zewail, A. H. *J. Phys. Chem. A* **xxxx**, **2002**, *106*, 9837.
- (2) Gouterman, M.; Wagnière, G. H.; Snyder, L. C. *J. Mol. Spectrosc.* **1963**, *11*, 108.

- (3) Dorough, G. D.; Miller, J. R.; Huennekens, F. M. *J. Am. Chem. Soc.* **1951**, *73*, 4315.
- (4) Quimby, D. J.; Longo, F. R. *J. Am. Chem. Soc.* **1975**, *97*, 5111.
- (5) Gradyushko, A. T.; Tsvirko, M. P. *Opt. Spectrosc. (USSR)* **1971**, *31*, 291.
- (6) Humphry-Baker, R.; Kalyanasundaram, K. *J. Photochem.* **1985**, *31*, 105.
- (7) Pekkarinen, L.; Linschitz, H. *J. Am. Chem. Soc.* **1960**, *82*, 2407.
- (8) Rodriguez, J.; Kirmaier, C.; Holten, D. *J. Am. Chem. Soc.* **1989**, *111*, 6500.
- (9) Bajema, L.; Gouterman, M.; Rose, C. B. *J. Mol. Spectrosc.* **1971**, *39*, 421.
- (10) Kotlo, V. N.; Solovyev, K. N.; Shkirman, S. F. *Izv. Akad. Nauk SSSR Ser. Fiz.* **1975**, *39*, 1972.
- (11) Tsvirko, M. P.; Stelmakh, G. F.; Pyatosin, V. E.; Solovyov, K. N.; Kachura, T. F. *Chem. Phys. Lett.* **1980**, *73*, 80.
- (12) Ohno, O.; Kaizu, Y.; Kobayashi, H. *J. Chem. Phys.* **1985**, *82*, 1779.
- (13) Kurabayashi, Y.; Kikuchi, K.; Kokubun, H.; Kaizu, Y.; Kobayashi, H. *J. Phys. Chem.* **1984**, *88*, 1308.
- (14) Stelmakh, G. F.; Tsvirko, M. P. *Opt. Spectrosc. (USSR)* **1983**, *55*, 516.
- (15) Even, U.; Magen, J.; Jortner, J.; Friedman, J.; Levanon, H. *J. Chem. Phys.* **1982**, *77*, 4374.
- (16) Chosrowjan, H.; Tanigichi, S.; Okada, T.; Takagi, S.; Arai, T.; Tokumaru, K. *Chem. Phys. Lett.* **1995**, *242*, 644.
- (17) Kishii, N.; Shirai, K.; Tamura, S.; Seto, J.; Tokumaru, K.; Takagi, S.; Arai, T.; Sakuragi, H. *J. Lumin.* **1995**, *64*, 125.
- (18) Vacha, M.; Machida, S.; Horie, K. *J. Phys. Chem.* **1995**, *99*, 13163.
- (19) Tokumaru, K. *J. Porphyrins Phthalocyanines* **2001**, *5*, 77.
- (20) Gurzadyan, G. G.; Tran-Thi, T.-H.; Gustavsson, T. *J. Chem. Phys.* **1998**, *108*, 385.
- (21) Gurzadyan, G. G.; Tran-Thi, T.-H.; Gustavsson, T. *Proc. SPIE—Int. Soc. Opt. Eng.* **2000**, *4060*, 96.
- (22) Kumble, R.; Palese, S.; Lin, V. S.-Y.; Therien, M. J.; Hochstrasser, R. M. *J. Am. Chem. Soc.* **1998**, *120*, 11489.
- (23) LeGourriérec, D.; Andersson, M.; Davidsson, J.; Mukhtar, E.; Sun, L. C.; Hammarström, L. *J. Phys. Chem. A* **1999**, *103*, 557.
- (24) Rodriguez, J.; Kirmaier, C.; Holten, D. *J. Chem. Phys.* **1991**, *94*, 6020.
- (25) Mataga, N.; Shibata, Y.; Chosrowjan, H.; Yoshida, N.; Osuka, A. *J. Phys. Chem. B* **2000**, *104*, 4001.
- (26) Yu, H. Z.; Baskin, J. S.; Steiger, B.; Wan, C. Z.; Anson, F. C.; Zewail, A. H. *Chem. Phys. Lett.* **1998**, *293*, 1.
- (27) Seely, G. R.; Calvin, M. *J. Chem. Phys.* **1955**, *23*, 1068.
- (28) Edwards, L.; Dolphin, D. H.; Gouterman, M.; Adler, A. D. *J. Mol. Spectrosc.* **1971**, *38*, 16.
- (29) Nappa, M.; Valentine, J. S. *J. Am. Chem. Soc.* **1978**, *100*, 5075.
- (30) Gouterman, M. In *The Porphyrins*; Dolphin, D., Ed.; Academic Press: New York, 1978; Vol. 3, p 1.
- (31) Seybold, P. G.; Gouterman, M. *J. Mol. Spectrosc.* **1969**, *31*, 1.
- (32) Harriman, A. *J. Chem. Soc., Faraday Trans. 2* **1981**, *77*, 1281.
- (33) Tobita, S.; Kaizu, Y.; Kobayashi, H.; Tanaka, I. *J. Chem. Phys.* **1984**, *81*, 2962.
- (34) Tobita, S.; Tanaka, I. *Chem. Phys. Lett.* **1983**, *96*, 517.
- (35) Kalyanasundaram, K. *Photochemistry of Polypyridine and Porphyrin Complexes*; Academic Press: London, 1992.
- (36) Galli, C.; Wynne, K.; LeCours, S. M.; Therien, M. J.; Hochstrasser, R. M. *Chem. Phys. Lett.* **1993**, *206*, 493.
- (37) Wynne, K.; LeCours, S. M.; Galli, C.; Therien, M. J.; Hochstrasser, R. M. *J. Am. Chem. Soc.* **1995**, *117*, 3749.
- (38) Wurzer, A. J.; Wilhelm, T.; Piel, J.; Riedle, E. *Chem. Phys. Lett.* **1999**, *299*, 296.
- (39) Akimoto, S.; Yamazaki, T.; Yamazaki, I.; Osuka, A. *Chem. Phys. Lett.* **1999**, *309*, 177.
- (40) Rodriguez, J.; Holten, D. *J. Chem. Phys.* **1989**, *91*, 3525.
- (41) Gustavsson, T.; Baldacchino, G.; Mialocq, J.-C.; Pommeret, S. *Chem. Phys. Lett.* **1995**, *236*, 587.
- (42) Strat, R. M.; Maroncelli, M. *J. Phys. Chem.* **1996**, *100*, 12981 and references therein.
- (43) Fajer, J.; Borg, D. C.; Forman, A.; Dolphin, D.; Felton, R. H. *J. Am. Chem. Soc.* **1970**, *92*, 3451.
- (44) Wan, C.; Fiebig, T.; Kelley, S. O.; Treadway, C. R.; Barton, J. K.; Zewail, A. H. *Proc. Natl. Acad. Sci. U.S.A.* **1999**, *96*, 6014.
- (45) Morandeira, A.; Engeli, L.; Vauthey, E. *J. Phys. Chem. A* **2002**, *106*, 4833.